Pure Appl. Chem., Vol. 85, No. 7, pp. 1451–1463, 2013.
http://dx.doi.org/10.1351/PAC-CON-12-10-28

A fluorescence study of the solute–solvent interactions of aminochalcones in a room-temperature ionic liquid*

Kotni Santhosh, G. Krishnamurthy Grandhi, Snigdha Ghosh, and Anunay Samanta‡

School of Chemistry, University of Hyderabad, Hyderabad 500046, India

Abstract: Unlike most other electron donor–acceptor (EDA) molecules, aminochalcones exhibit unusual solvent polarity-dependent fluorescence behavior. The photophysical behavior of two aminochalcones, namely, 4-aminochalcone (AC) and 4-dimethylaminochalcone (DMAC), has been studied in a viscous room-temperature ionic liquid (IL), 1-butyl-3-methylimidazolium hexafluorophosphate, [bmim][PF_6], by steady-state and time-resolved fluorescence techniques. The observation of a single emission band in viscous IL, which is similar to the one observed in less viscous polar conventional solvents, suggests no twisting is necessary for the formation of the charge-transfer state from which the emission of aminochalcones originates. The fluorescence decay profiles, solvation dynamics, and excitation-wavelength-dependent emission behavior of AC are found to be quite different from those of DMAC in the IL. The observed difference is attributed to specific H-bonding interaction between AC and [bmim][PF_6].

Keywords: aminochalcones; excited state; fluorescence spectroscopy; ionic liquids; solute–solvent interactions; steady-state and time-resolved fluorescence.

INTRODUCTION

Room-temperature ionic liquids (ILs) are now widely studied in many areas of chemistry and biology, as evidenced by the large and rapidly increasing number of recent publications devoted to understanding and exploiting their distinctive properties. These are of particular relevance in pursuit of green chemistry objectives [1,2] and new applications in materials science and biology [3–6]. These novel materials also offer new challenges and opportunities in physical chemistry. Several experimental and theoretical measurements have been performed to characterize these materials. Electrochemical, thermodynamic, and photophysical studies such as solvation and rotational dynamics and electron- and proton-transfer reactions carried out on the ILs have contributed to the better understanding of the effect of microviscosity, micropolarity, and ionicity of these materials on the chemical reactions [7–19].

Electron donor–acceptor (EDA) molecules have attracted the attention of researchers because of their potential applications in several areas [20–22]. Photoinduced charge separation in EDA molecules is the basis of design and development of systems for solar energy conversion [23,24], luminescent systems for sensing environments [25], nanometer-scale wires and logic gates [26–28], and also for mak-

Pure Appl. Chem.* **85, 1257–1513 (2013). A collection of invited papers based on presentations at the XXIVth IUPAC Symposium on Photochemistry, Coimbra, Portugal, 15–20 July 2012.
‡Corresponding author: Fax: (+91)4023011594; E-mail: assc@uohyd.ernet.in, anunay.samanta@gmail.com

ing components of molecular electronic devices [29]. The EDA molecules commonly emit from an intramolecular charge-transfer (ICT) state, which is most often more polar than the ground state. Several families of EDA molecules have been studied extensively, and in most of the cases, a decrease in fluorescence quantum yield and lifetime is observed with increase in solvent polarity [30,31]. In this work, we concentrate on the photophysics of aminochalcones, which contain an amino/dimethylamino group as an electron donor and a carbonyl group as an acceptor (Fig. 1). These systems exhibit fluorescence behavior that is not common for the EDA systems. The fluorescence quantum yield and lifetimes of aminochalcones increase with increase in polarity of the medium. Stilbenes [32], flavones [33], and thiazoloquinoxalines [34] are a few other EDA molecules of this category. It is necessary to consider multiple close-lying excited states to explain the unusual solvent dependence of the fluorescence behavior of such EDA molecules. The number of these excited states varies from system to system. For example, a three-state model in the case of stilbenes [32] and a two-state model in the case of flavone derivatives [33] are proposed.

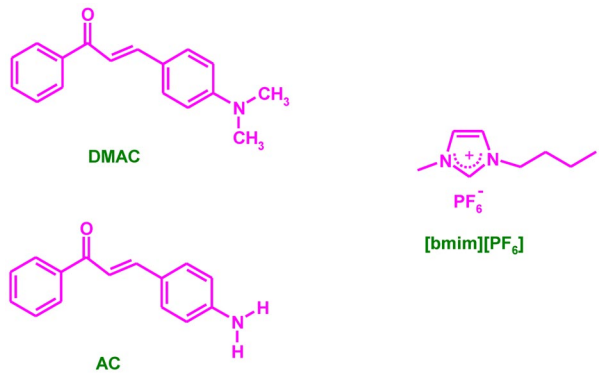

Fig. 1 Structures of DMAC, AC, and [bmim][PF_6] employed in this study.

The excited-state mechanism of aminochalcones was deduced by comparing the photophysical properties of these systems with those of the stilbene derivatives and bridged compounds of chalcones [35–37]. The currently accepted understanding is that the chalcone derivatives are present in their *trans* (*E*) form in the ground state. On photoexcitation, the molecule can undergo *trans–cis* isomerization and/or ICT from donor (amino moiety) to acceptor (keto group) depending on the nature of the medium. In nonpolar solvents, these molecules emit weakly from their E^* state [35,36]. Competing *trans* $\rightarrow$ *cis* ($E^* \rightarrow Z^*$) isomerization is believed to be responsible for the weak fluorescence in nonpolar solvents [36]. In more polar media, the molecule emits more strongly from the dialkylanilino twisted ICT (TICT) state, which is commonly termed as A^* state [35,36]. Scheme 1 illustrates the formation of A^* state from the locally excited E^* state as a function of the polarity of the medium.

Fluorescence behavior of aminochalcones is particularly sensitive to polarity and viscosity of the medium, and it is therefore interesting to explore whether such behavior can be modulated in response to these distinctive properties of ILs. Polarity of the IL favors the emission from A^* state, whereas the high viscosity of the IL is likely to slow down the transformation of the A^* state from the E^* state. In order to gain insight into the opposing effects of the viscosity and polarity of the ILs we have studied photophysical properties of 4-aminochalcone (AC) and 4-dimethylaminochalcone (DMAC) in 1-butyl-3-methylimidazolium hexafluorophosphate, [bmim][[PF_6] IL (Fig. 1). DMAC has been the subject of previous studies in conventional solvents but, to the best of our knowledge, this is a first study involving the photophysics of AC. We have chosen [bmim][PF_6] in this work because of its optical purity, high viscosity, and polarity.

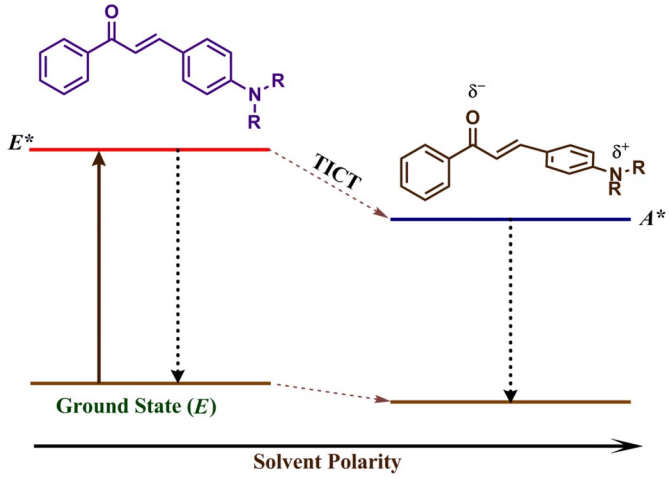

Scheme 1 Excited-state ICT mechanism of aminochalcones.

EXPERIMENTAL

Materials

Acetophenone, 4-dimethylaminobenzaldehyde, 4-bromobenzaldehyde, *N*-methyl-2-pyrrolidone (NMP), and aqueous solution of ammonia used for synthesis of AC and DMAC were purchased from local companies. The aminochalcones were synthesized following reported procedures for AC [38] and DMAC [39]. The IL, [bmim][PF_6] (Fig. 1), used in this study was procured from Kanto Chemicals (Japan). The IL was kept under vacuum for several hours prior to use. Laser-grade coumarin 153 (C153) for quantum yield measurements was purchased from Eastman Kodak and used as received. Acetonitrile as solvent for quantum yield measurements was procured from Merck and was dried by following reported procedure prior to spectral measurements [40].

Instrumentation and methods

The viscosity of [bmim][PF_6] was measured by an LVDV-III Ultra Brookfield cone and plate viscometer (accuracy: ±1 %). The absorption and steady-state fluorescence spectra were recorded on a UV–vis spectrophotometer (Cary 100, Varian) and spectrofluorimeter (Fluorolog-3, Jobin Yvon), respectively. The fluorescence spectra were corrected for the instrument response. Time-resolved fluorescence measurements at room temperature (RT, 296 K) and 273 K were carried out using a time-correlated single-photon counting (TCSPC) spectrometer (Horiba Jobin Yvon IBH). PicoBrite diode laser source (λ_{exc} = 405 nm) was used as the excitation source and an MCP photomultiplier (Hamamatsu R3809U-50) as the detector. The pulse repetition rate of the laser source was 10 MHz. The instrument response function, which was limited by the full width half maximum (fwhm) of the excitation pulse, was 50 ps. The lamp profile was recorded by placing a scatterer (dilute solution of Ludox in water) in place of the sample. The time-resolved emission decay profiles were collected at 5/10 nm intervals across the steady-state emission spectrum. The wavelength selection was made by a monochromator with a band-pass of 2/4 nm. Decay curves were analyzed by nonlinear least-squares iteration procedure using IBH DAS6 (version 2.2) decay analysis software. The quality of the fit was assessed by the inspection of the chi-square (χ^2, a measure of mis-match between original and fitted data) values and distribution of the residuals. The time-resolved emission spectra (TRES) were constructed following a standard procedure [41]. The frequencies corresponding to the emission maxima were obtained by fitting the emission profiles to a log-normal function given by the following equation [42]:

$$F(\bar{\nu},t) = h\exp\left\{-\ln(2)\left[\ln(1+\alpha)/\gamma\right]^2\right\}, \quad \text{for } \alpha > -1$$
$$= 0 \quad \text{for } \alpha \le -1 \tag{1}$$
$$\alpha = 2\gamma\left[\bar{\nu} - \bar{\nu}_p\right]/\Delta$$

where h is the peak height, $\bar{\nu}_p$ is the peak frequency, γ is the asymmetry parameter, and Δ is the width of the curve. Nonlinear least squares fitting was used to obtain the best fitted curves until successive iterations gave identical χ^2 value.

The change in the dipole moment of the molecules on electronic excitation was estimated by following the Stokes shift ($\Delta\bar{\nu} = \bar{\nu}_a - \bar{\nu}_f$) of the fluorophore as a function of polarity (E_T^N) of the medium [43].

$$\left(\bar{\nu}_a - \bar{\nu}_f\right) = 11307.6\left\{\left(\Delta\mu/\Delta\mu_D\right)^2\left(a_D/a\right)^3\right\}E_T^N + \text{constant} \tag{2}$$

where $\bar{\nu}_a$ and $\bar{\nu}_f$ represent peak frequencies of absorption and emission maxima. $\Delta\mu$ and a denote dipole moment change and Onsager cavity radius, respectively, of the fluorophore. Density functional theory (DFT) calculations were performed with B3LYP/6-311+G(d) level of theory in dichloromethane using the GAUSSIAN09 program package [44] for the measurement of Onsager cavity radii. The measured values are 5.70 and 5.08 Å for DMAC and AC, respectively. $\Delta\mu_D$ and a_D represent the dipole moment change and the Onsager cavity radius of the betaine dye, respectively.

Fluorescence quantum yields of the chalcone derivatives were measured using coumarin 153 (C153) as the reference compound ($\Phi_f = 0.56$ in acetonitrile) [45]. Optically matched solutions of the sample and reference at the excitation wavelength were used for the quantum yield measurements. The quantum yields were estimated using the relation [46]

$$\phi_{sample} = \phi_{std}\left[\frac{I_{sample} \times \text{O.D}_{std} \times n_{sample}^2}{I_{std} \times \text{O.D}_{sample} \times n_{std}^2}\right] \tag{3}$$

where ϕ, I, O.D, and n represent the fluorescence quantum yield, total fluorescence intensity (area under the fluorescence curve), optical density, and refractive index, respectively.

Solvation time ($\bar{\tau}_{solv}$) was estimated by fitting $\bar{\nu}(t)$ against t using the following equation [47–49]:

$$\bar{\nu}(t) = \bar{\nu}(\infty) + \Delta\bar{\nu}\exp\left[-\left(\frac{t}{\tau_0}\right)^{\beta}\right] \tag{4}$$

where $0 < \beta \le 1$, and

$$\bar{\tau}_{solv} = \frac{\tau_0}{\beta}\Gamma\left(\beta^{-1}\right) \tag{5}$$

where Γ is the gamma function.

The actual time-zero spectrum was calculated following a reported procedure [50].

$$\bar{\nu}(0)_{calc} = \left(\bar{\nu}_{abs}^{max}\right)_p - \left[\left(\bar{\nu}_{abs}^{max}\right)_{np} - \left(\bar{\nu}_{em}^{max}\right)_{np}\right] \tag{6}$$

where $(\bar{\nu}_{abs}^{max})_p$ represents absorption maximum of the fluorophore in polar solvent, $(\bar{\nu}_{abs}^{max})_{np}$ and $(\bar{\nu}_{em}^{max})_{np}$ represent absorption and emission maxima of the same fluorophore in nonpolar solvent. In the present experiments, [bmim][PF_6] is the polar solvent and hexane is the nonpolar solvent.

RESULTS

The steady-state absorption and emission spectral behavior of DMAC and AC is measured in conventional nonpolar and polar solvents, and the spectral data, ϕ_f and $\bar{\tau}$ values are collected in Table 1. An enhancement of the ϕ_f and $\bar{\tau}$ values of these molecules is observed with increase in the solvent polarity. The ϕ_f values presented in Table 1 indicate that DMAC is more fluorescent than AC. The red shift of the emission maximum with increase in solvent polarity is consistent with the charge-transfer nature of the emitting state. The steady-state spectral behavior of the systems in [bmim][PF_6] (shown in Fig. 2) is compared to that in conventional solvents. The absorption and emission spectral maxima of the compounds in IL are red-shifted relative to that in conventional solvents, indicating that spectral positions are dependent on the polarity of the medium. This is consistent with the ICT nature of the excited state of the molecules. That the ICT character of the emission increases with increase in inductive influence of the donor group is evident from the large red shift of the absorption and emission maxima of DMAC compared to AC in all the solvents.

Table 1 Comparison of the steady-state spectral data and fluorescence lifetimes of DMAC and AC in conventional solvents and [bmim][PF_6] at 296 K.

Solvent (E_T^N)	λ_{max}^{abs}/nm		λ_{max}^{em}/nm		Φ_f /10^{-3}		$\bar{\tau}$/ps	
	AC	DMAC	AC	DMAC	AC	DMAC	AC	DMAC
Toluene (0.099)	368	405	444	465	–	11.0	<50	90
1,4-Dioxane (0.111)	370	405	462	480	2.5	30.0	<50	220
$CHCl_3$ (0.259)	375	410	475	505	4.6	66.0	70	480
DCM (0.309)	376	415	485	515	5.3	153.0	100	1120
Acetone (0.355)	380	418	500	520	30.0	265.0	270	1550
DMSO (0.444)	406	425	527	555	113.0	206.0	450	1140
Acetonitrile (0.460)	383	410	506	540	38.0	186.0	290	930
[bmim][PF_6] (0.676)	388	420	512	550	100.0	190.0	1200	1400

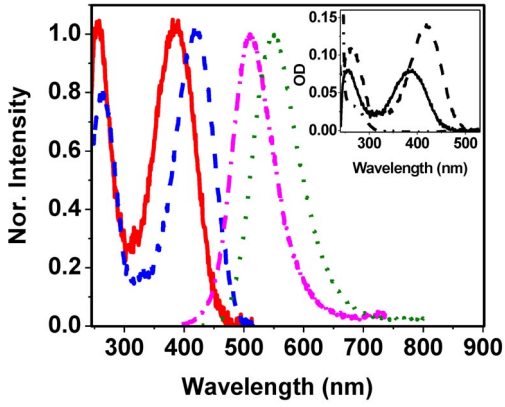

Fig. 2 Normalized absorption spectra of AC (solid line), DMAC (dashed line), and emission spectra of AC (dash-dot line), DMAC (dotted line) in [bmim][PF_6]. Inset shows the absorption spectrum of the [bmim][PF_6] (dash-dot-dot) along with the absorption spectra of AC and DMAC highlighting the optical transparency of the IL. All the spectra were recorded with air as reference.

It was earlier proposed that the charge-transfer state is associated with TICT conformation [35–37]. As aminochalcones have so far been studied only in less viscous conventional solvents, the

role of viscosity on the photophysics of these molecules is not yet explored. In a highly viscous environment, as the twisting of the dialkylanilino group is expected to be retarded (Scheme 1) one can expect emission from the E^* state despite the polar nature of the media. However, Fig. 2 shows a single emission band in highly viscous and polar [bmim][PF_6], which is similar to the reported A^* emission in conventional solvents.

Figure 3 shows emission-wavelength-dependent fluorescence decay profiles and normalized TRES of DMAC in [bmim][PF_6] at room temperature (296 K) and 273 K. TRES at both the temperatures represent single emission maxima. The rise of the fluorescence intensity followed by a decay behavior at the longer emitting wavelengths is a manifestation of the slow solvation dynamics of the fluorescent state of the DMAC in [bmim][PF_6]. As shown in Fig. 4, solvation times are estimated by fitting the data to stretched exponential equation (see experimental section). With decrease in temperature an increase in the solvation time is evident from Fig. 4 and Table 2. The spectrum with dotted line in Fig. 3 represents time-zero spectrum estimated following the procedure outlined in the experimental section. The calculated time-zero emission maximum $\bar{\nu}(0)_{calc}$ deviates from the value ($\bar{\nu}(0)_{exp}$) estimated from the experimental data. As shown in Table 2, the magnitudes of the shift ($\bar{\nu}(0)_{calc} - \bar{\nu}(0)_{exp}$) of time-zero emission maxima of DMAC at 296 and 273 K are minimal and the calculated missing components of the solvation dynamics in [bmim][PF_6] are 25 and 21 % at 296 and 273 K, respectively, which are in accordance with the reported missing components of the solvation dynamics in highly viscous ILs [51].

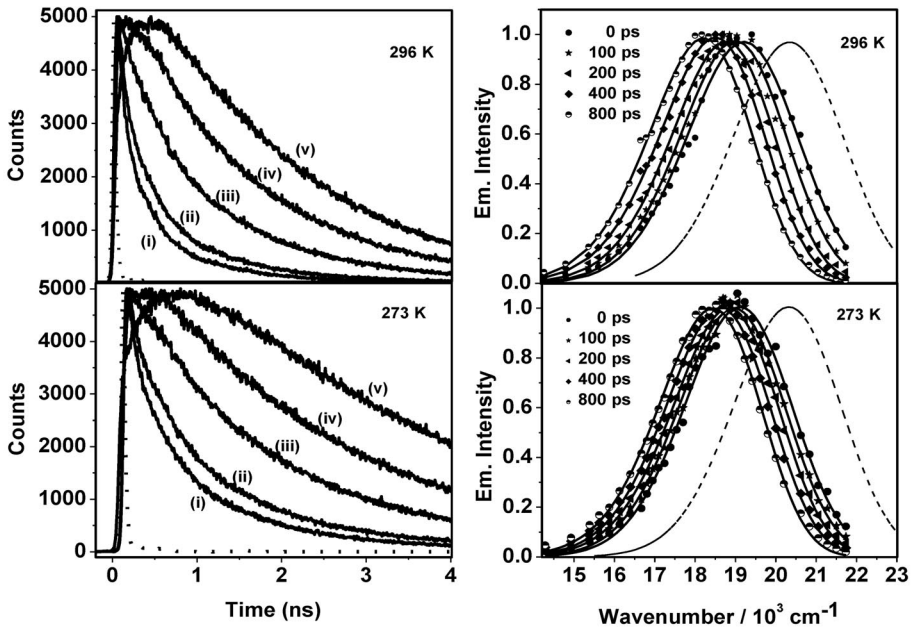

Fig. 3 Emission-wavelength-dependent fluorescence decay profiles of DMAC (left panel) in [bmim][PF_6] at 296 and 273 K. The monitoring wavelengths are (i) 490, (ii) 500, (iii) 525, (iv) 550, and (v) 600 nm. Lamp profile is shown as dotted line. Normalized TRES of DMAC in [bmim][PF_6] at different delay times are shown in the right panel. Spectrum with dotted line represents the estimated time-zero spectrum. λ_{exc} = 405 nm.

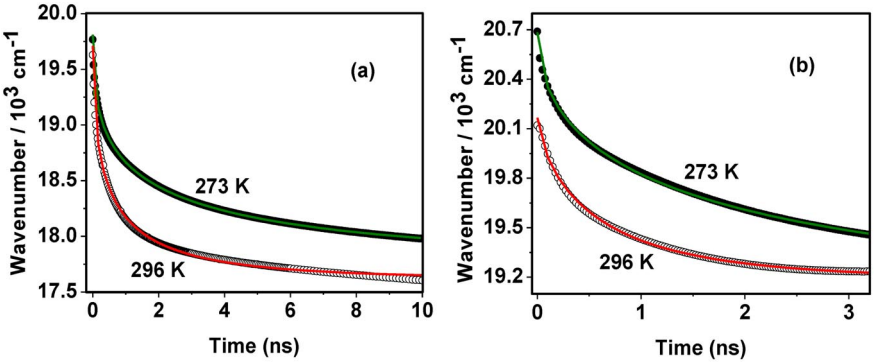

Fig. 4 Stretched exponential fit to the solvation data in [bmim][PF_6] at 273 and 296 K for DMAC (a) and AC (b).

Table 2 Time-resolved fluorescence spectral data of DMAC and AC in [bmim][PF_6] at 296 and 273 K.

Temp.	Sample	$\bar{\nu}(0)_{calc} - \bar{\nu}(0)_{exp}$/cm^{-1}	$\bar{\nu}(0)_{exp} - \bar{\nu}(\infty)$/cm^{-1}	$\bar{\nu}(0)_{calc} - \bar{\nu}(\infty)$/cm^{-1}	Missing component	$\bar{\tau}_{solv}$/ns
296 K	DMAC	670	2013	2683	25 %	1.2
	AC	2810	884	3694	76 %	0.6
273 K	DMAC	532	2055	2587	21 %	5.5
	AC	2240	1370	3610	62 %	1.2

Though TRES of AC also characterized with single emission maximum (Fig. 5), fluorescence decay profiles and TRES data of AC are quite different from those of DMAC. Unlike DMAC, at the two different temperatures (296 and 273 K), no rise for the emission intensity-time profile of AC is noticed at longer emitting wavelengths. The stretched exponential fit to the solvation data of AC is shown in Fig. 4. From Table 2, it is clear that the $\bar{\tau}_{solv}$ values of AC are much less than those of DMAC at both temperatures and values of the shift in time-zero emission maximum ($\bar{\nu}(0)_{calc} - \bar{\nu}(0)_{exp}$) of AC are high compared to DMAC. The missing components estimated using the experimental and calculated time-dependent Stokes shift ($\bar{\nu}(0) - \bar{\nu}(\infty)$) values are exceptionally high and 76 % at 296 K decreases to 62 % at 273 K.

Even though in conventional less viscous solvents the chalcone derivatives do not display excitation-wavelength-dependent emission behavior, both DMAC and AC are found to display excitation-wavelength-dependent emission behavior, when excited at the red side of the absorption spectra in [bmim][PF_6]. Figure 6 shows the excitation-wavelength-dependent shift in the emission maxima of these molecules at different temperatures and their excitation spectra at 296 K. The magnitudes of the λ_{exc}-dependent red shift of the spectral maxima of DMAC and AC measured at three different temperatures (273, 296, and 323 K) are compared (Table 3). DMAC shows a red shift of 12 nm at 273 K, which decreases gradually to 6 nm at 296 K and 3 nm at 323 K. AC also shows a similar trend in the temperature range of 273 to 296 K (shift from 11 to 7 nm), but behaves quite differently at higher temperature region, 296 to 323 K. Unlike DMAC, the spectral shift exhibited by AC is found independent of the temperature in the entire region from 296 to 323 K (Table 3).

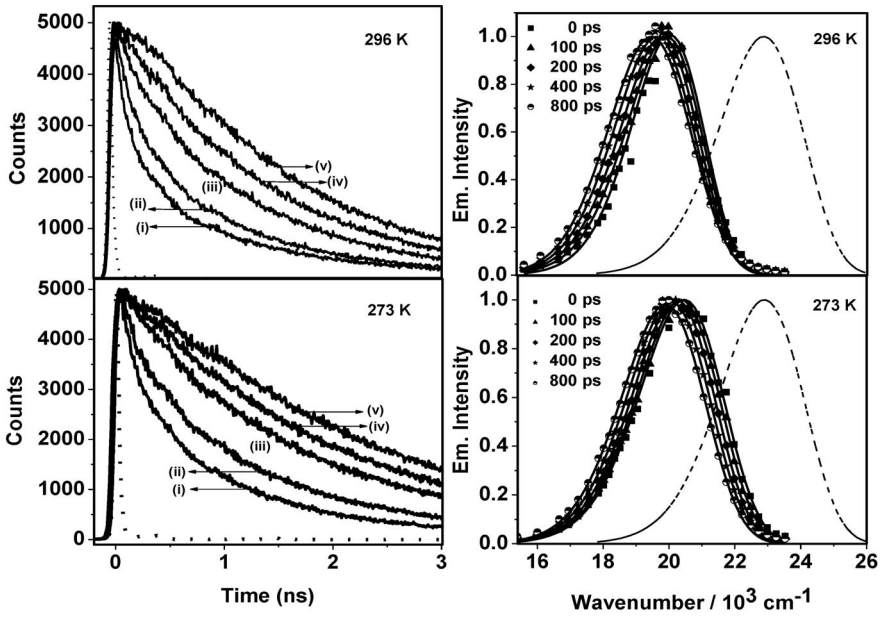

Fig. 5 Emission-wavelength-dependent fluorescence decay profiles of AC (left panel) in [bmim][PF_6] at 296 and 273 K. The monitoring wavelengths are (i) 475, (ii) 490, (iii) 515, (iv) 535, and (v) 580 nm. Lamp profile is shown as dotted line. Normalized TRES of AC in [bmim][PF_6] at different delay times are shown in the right panel. Spectrum with dotted line represents the estimated time-zero spectrum. λ_{exc} = 405 nm.

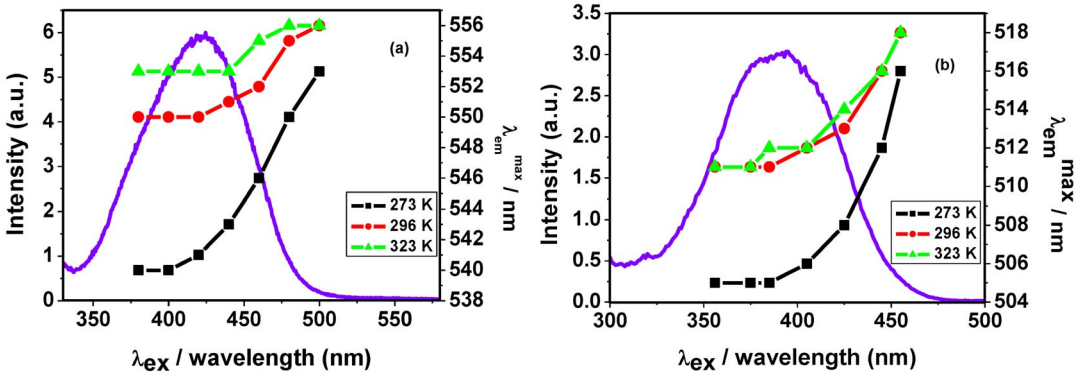

Fig. 6 λ_{em}^{max} vs. λ_{ex} plots of DMAC (a) and AC (b) in [bmim][PF_6] at three different temperatures. Excitation spectra of the compounds at 296 K are also shown.

Table 3 Excitation-wavelength-dependent shift of the fluorescence maxima of DMAC and AC in [bmim][PF_6] at different temperatures.

Sample	Temp./K	Shift of the fluorescence maximum/nm	$\bar{\tau}_{solv}$/ns	$\bar{\tau}$/ns
DMAC in [bmim][PF_6]	273	12	5.5	2.00
	296	6	1.2	1.40
	323	3	–	0.70
AC in [bmim][PF_6]	273	11	1.2	1.90
	296	7	0.6	1.20
	323	7	–	0.62

DISCUSSION

Number and nature of the state

The data presented in Table 1 and spectral features depicted in Fig. 2 clearly show that the emission of aminochalcones, DMAC and AC, originates only from a single charge-transfer state. The time-resolved fluorescence measurements not only substantiate this but they also provide insights into the nature of this state. Despite high viscosity (285 cP) of [bmim][PF_6] at 296 K, the TRES of DMAC did not show any second emission component at room temperature. Even at a much lower temperature, 273 K, when [bmim][PF_6] is in its semisolid form, one anticipates a further slowdown of the twisting of a large moiety, which is necessary for the formation of A^* state, and expects emission largely from the E^* state with small or negligible contribution from the A^* state. However, this is not the case. Figure 3 shows a single emission maximum even at low temperature. The findings are very similar for AC as well. Lack of dual emission in the TRES of the two compounds at room or low temperature unambiguously establishes that these molecules emit only from a single state, which can be the A^* state formed due to ultrafast $E^* \rightarrow A^*$ transformation (even in highly viscous medium) or the E^* state, which does not require any twisting.

According to the literature, aminochalcones emit from the E^* state in nonpolar solvents and from A^* state in highly polar solvents [35,36]. However, if this were indeed the case, one would have observed some separation of the two emission bands with change in polarity of the medium. However, as shown in Fig. 7, this is not the case. The spectra in conventional solvents represent only one emission, which shows solvatochromic shift. The inset of Fig. 7 shows the variation of the emission maximum with the polarity (E_T^N) of the medium. Had there been a change in the nature of the emitting state with variation of the polarity of the medium, there would have been a departure from the linear relationship, which is observed here. That the fluorescent state of the molecule is not associated with twisting of the dialkylanilino group is also evident from the change of dipole moment ($\Delta\mu = \mu_E - \mu_G$) on excitation. From the plots of Stokes shift ($\bar{\nu}_a - \bar{\nu}_f$) vs. ($E_T^N$) for both DMAC and AC (shown in Fig. 8), the estimated $\Delta\mu$ values of DMAC and AC are 6.2 and 4.6 D, respectively. The $\Delta\mu$ value of the former, which is known already, is close to the estimated value [35,36]. This change is too small to be explained in terms of the TICT model, particularly when the large distance of separation of the charge centers are taken into consideration. For example, even for a small molecule like 4-(*N*,*N*′-dimethylamino) benzonitrile (DMABN) or crystal violet lactone (CVL), where the TICT mechanism was invoked, the $\Delta\mu$ values (16 and 20 D) [52–54] are much higher than that for the present system. One can also use more line of arguments to come to the same conclusion. Firstly, the linearity of the plots clearly rules out any possibility of either the change of the nature of the state with polarity or involvement of the multiple states as found in some cases [31,55]. Secondly, had there been any involvement of the multiple fluorescent states, the fluorescence decay profiles would have been multi-exponential in nature. However, the sin-

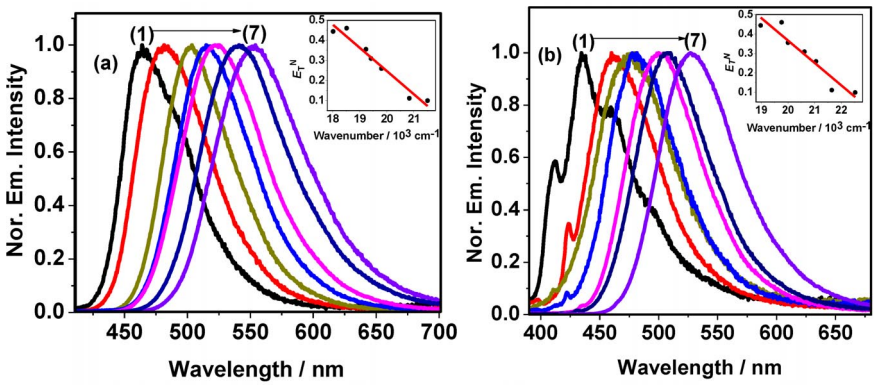

Fig. 7 Emission spectra of DMAC (a) and AC (b) in different nonpolar and polar solvents. Solvents from (1) to (7) are toluene, dioxane, $CHCl_3$, DCM, acetone, acetonitrile, and DMSO. E_T^N vs. emission maximum (in cm^{-1}) plots are shown as insets.

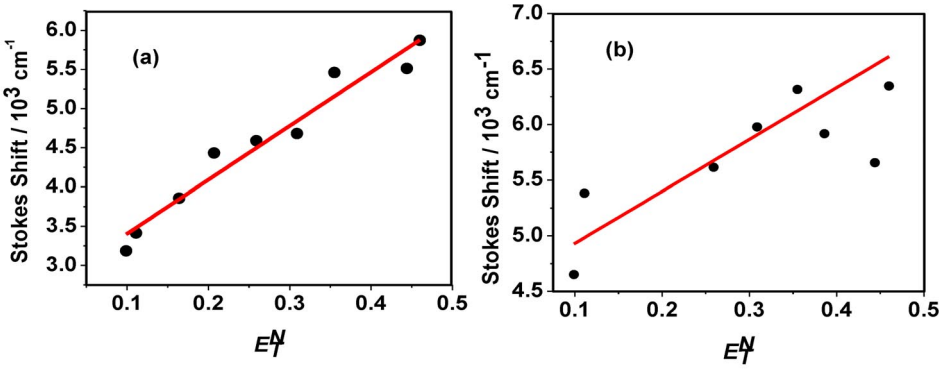

Fig. 8 Stokes shift vs. E_T^N plots of DMAC (a) and AC (b) in different solvents of different polarities.

gle-exponential nature of the fluorescence decay profiles, as observed for the present systems, clearly points to the involvement of a single emitting state, which is clearly shown to be not the A^* state.

Contrasting behavior of AC and DMAC

It is interesting to note the large difference of the fluorescence decay profiles and TRES of two structurally similar aminochalcones. The decay profiles of AC did not show any rise with time as observed in the case of DMAC. The time-dependent shift of the emission spectra could be observed more clearly only in the case of DMAC. It is evident from the data that this difference is the result of significantly faster solvent relaxation of the fluorescent state of AC compared to DMAC. This aspect, i.e., a faster solvation of AC, is also evident from the shift of actually observed time-zero spectrum from the expected time-zero spectrum. The difference in the peak frequencies of these two spectra, which is the result of fast solvation dynamics compared to the time resolution of the set-up and is termed as the "missing component" of the solvent relaxation, is much higher (76 and 62 % at 296 and 273 K, respectively) in the case of AC compared to DMAC, clearly indicating that solvent relaxation of the fluorescence state of former system is much faster.

A faster solvation dynamics of AC in [bmim][PF_6] can be understood considering the specific solute–solvent interactions. Maroncelli and co-workers have shown that molecules that are engaged in

H-bonding interaction with the solvent are characterized by faster solvation times than those that do not interact with the solvent molecules through specific interactions [56]. Studies on H-bonding interactions between solute and IL, and their effect on solute rotation and solvation dynamics, have also been reported in the literature [14,15,51,57]. As the amino hydrogens of AC can involve in the H-bonding interactions with $[PF_6]^-$ of the IL, whereas DMAC cannot, the specific solute–solvent interaction can be considered as the factor responsible for faster solvation of AC in [bmim][PF_6]. This specific H-bonding interaction of AC with [bmim][PF_6] can also be used to understand the difference in the excitation wavelength dependence of the emission behavior of the two compounds in [bmim][PF_6]. At room temperature (296 K), DMAC and AC show an excitation-wavelength-dependent emission spectral shift of 6 and 7 nm, respectively (Table 3 and Fig. 6) [58]. A comparable solvation time and fluorescence lifetime of DMAC at 296 K makes it understandable why it exhibits excitation-wavelength-dependent emission behavior. However, as the solvation time of AC is less than its fluorescence lifetime, the excitation-wavelength-dependent emission behavior of this system cannot be explained comparing the time scale of solvation time and fluorescence lifetime. To understand the origin of the excitation-wavelength-dependent emission spectra of AC, experiments have been carried out at lower (273 K) and higher (323 K) temperatures (Fig. 6). Table 3 compares the solvation and fluorescence lifetimes of DMAC and AC at different temperatures. At lower temperature (273 K) as the solvation time (5.5 ns) of DMAC is significantly higher than its fluorescence lifetime (2.00 ns), one observes emission from incompletely solvated state giving rise to a greater excitation wavelength dependence. At higher temperature (323 K), as the solvation time of DMAC is lower than its fluorescence lifetime, the excitation-wavelength-dependent spectral shift becomes less pronounced. However, as the solvation times of AC are lower than the fluorescence lifetime at all working temperatures, its excitation wavelength dependence should not be due to the emission from incompletely solvated states. It is well known that H-bonding interaction between the solute and solvent also gives rise to excitation-wavelength-dependent fluorescence behavior [59]. As AC is involved in the H-bonding interaction with $[PF_6]^-$, it is this factor that contributes to the excitation wavelength dependence of this molecule in [bmim][PF_6].

CONCLUSION

The present study reveals an interesting difference of the photophysical behavior of two structurally similar aminochalcones in [bmim][PF_6] IL. The nature of the emitting state in these compounds is also found to be different from the commonly accepted model. It is concluded that the emission of aminochalcones in polar environment (including IL) originates from a dipolar state which does not require any twisting. The fluorescence decay profiles, solvation dynamics, and excitation-wavelength-dependent emission behavior of DMAC are found to be quite different from those of AC. A faster solvation dynamics and greater excitation wavelength dependence of the emission behavior of AC are attributed to specific H-bonding interactions of this compound with the IL.

ACKNOWLEDGMENTS

This work is supported by the J.C. Bose Fellowship (to A.S.) of the Department of Science and Technology, Government of India. We thank Dr. Tanmay Chatterjee for his help during the DFT calculations. Thanks are due to the Council of Scientific and Industrial Research for a Senior Research Fellowship to K.S.

REFERENCES

1. K. R. Seddon. *Ionic Liquids, Industrial Applications for Green Chemistry*, American Chemical Society, Washington, DC (2002).
2. J. P. Hallett, T. Welton. *Chem. Rev.* **111**, 3508 (2011).
3. H. Itoh, K. Naka, Y. Chujo. *J. Am. Chem. Soc.* **126**, 3026 (2004).
4. L. X. Yang, Y. J. Zhu, W. W. Wang, H. Tong, M. L. Ruan. *Angew. Chem., Int. Ed.* **43**, 1410 (2004).
5. K. Fujita, H. Ohno. *Biopolymers* **93**, 1093 (2010).
6. Z. Yuanyuan, C. Xiang, L. Jingbo, Y. Jingsong, C. Lijuan. *Chem. Biol. Drug Design* **74**, 282 (2009).
7. B. M. Quinn, Z. Ding, R. Moulton, A. J. Bard. *Langmuir* **18**, 1734 (2002).
8. A. Samanta. *J. Phys. Chem. Lett.* **1**, 1557 (2010).
9. A. Paul, A. Samanta. *J. Phys. Chem. B* **112**, 947 (2008).
10. A. Samanta. *J. Phys. Chem. B* **110**, 13704 (2006).
11. R. Karmakar, A. Samanta. *J. Phys. Chem. A* **106**, 6670 (2002).
12. S. N. V. K. Aki, J. F. Brennecke, A. Samanta. *Chem. Commun.* 413 (2001).
13. E. W. Castner, C. J. Margulis, M. Maroncelli, J. F. Wishart. *Ann. Rev. Phys. Chem.* **62**, 85 (2011).
14. S. K. Das, M. Sarkar. *Chem. Phys. Lett.* **515**, 23 (2011).
15. S. K. Das, M. Sarkar. *J. Phys. Chem. B* **116**, 194 (2012).
16. J. N. C. Lopes, A. A. H. Pauda. *J. Phys. Chem. B* **110**, 3330 (2006).
17. J. Guo, G. A. Baker, P. C. Hillesheim, S. Dai, R. W. Shaw, S. M. Mahurin. *Phys. Chem. Chem. Phys.* **13**, 12395 (2011).
18. D. K. Sasmal, A. K. Mandal, T. Mondal, K. Bhattacharyya. *J. Phys. Chem. B* **115**, 7781 (2011).
19. K. Iwata, H. Okajima, S. Saha, H.-O. Hamaguchi. *Acc. Chem. Res.* **40**, 1174 (2007).
20. C.-H. Yang, S.-H. Liao, Y.-K. Sun, Y.-Y. Chuang, T.-L. Wang, Y.-T. Shieh, W.-C. Lin. *J. Phys. Chem. C* **114**, 21786 (2010).
21. B. P. Rand, J. Xue, S. Uchida, S. R. Forrest. *J. Appl. Phys.* **98**, 124902 (2005).
22. A. Bard, M. A. Fox. *Acc. Chem. Res.* **28**, 141 (1995).
23. D. Bi, F. Wu, Q. Qu, W. Yue, Q. Cui, W. Shen, R. Chen, C. Liu, Z. Qiu, M. Wang. *J. Phys. Chem. C* **115**, 3745 (2011).
24. T. Kawatsu, V. Coropceanu, A. Ye, J.-L. Bredas. *J. Phys. Chem. C* **112**, 3429 (2008).
25. J.-H. Huang, W.-H. Wen, Y.-Y. Sun, P.-T. Chou, J.-M. Fang. *J. Org. Chem.* **70**, 5827 (2005).
26. A. P. de Silva, Y. Leydet, C. Lincheneau, N. D. McClenaghan. *J. Phys.: Condens. Matter* **18**, S1847 (2006).
27. J.-M. Montenegro, E. Perez-Inestrosa, D. Collado, Y. Vida, R. Suau. *Org. Lett.* **6**, 2401 (2004).
28. M. Andersson, L. E. Sinks, R. T. Hayes, Y. Zhao, M. R. Wasielewski. *Angew. Chem., Int. Ed.* **42**, 3139 (2003).
29. M. Kondratenko, A. G. Moiseev, D. F. Perepichka. *J. Mater. Chem.* **21**, 1470 (2011).
30. T. Soujanya, R. W. Fessenden, A. Samanta. *J. Phys. Chem.* **100**, 3507 (1996).
31. S. Saha, A. Samanta. *J. Phys. Chem. A* **106**, 4763 (2002).
32. R. Lapouyade, K. Czeschka, W. Majenz, W. Rettig, E. Gilabert, C. Rulliere. *J. Phys. Chem.* **96**, 9643 (1992).
33. M. Sarkar, R. K. Kanaparthi, B. Bhattacharya, A. Samanta. *J. Phys. Chem. A* **112**, 3302 (2008).
34. M. Shaikh, J. Mohanty, P. K. Singh, A. C. Bhasikuttan, R. N. Rajule, V. S. Satam, S. R. Bendre, V. R. Kanetkar, H. Pal. *J. Phys. Chem. A* **114**, 4507 (2010).
35. P. Wang, S. Wu. *J. Photochem. Photobiol., A* **86**, 109 (1995).
36. K. Rurack, M. L. Dekhtyar, J. L. Bricks, T. Resch-Genger, W. Rettig. *J. Phys. Chem. A* **103**, 9626 (1999).
37. Y.-B. Jiang, X.-J. Wang. *J. Photochem. Photobiol., A* **81**, 205 (1994).
38. H. Xu, C. Wolf. *Chem. Commun.* 3035 (2009).

39. X. T. Tao, T. Watanabe, K. Kono, T. Deguchi, M. Nakayama, S. Miyata. *Chem. Mater.* **8**, 1326 (1996).
40. D. D. Perrin, W. L. F. Armerego, D. R. Perrin. *Purification of Laboratory Chemicals*, Pergamon Press, New York (1980).
41. J. R. Lakowicz. *Principles of Fluorescence Spectroscopy*, 2nd ed., Kluwer Academic/Plenum Press, New York (1999).
42. M. L. Horng, J. A. Gardecki, A. Papazyan, M. Maroncelli. *J. Phys. Chem.* **99**, 17311 (1995).
43. M. Ravi, A. Samanta, T. P. Radhakrishnan. *J. Phys. Chem.* **98**, 9133 (1994).
44. M. J. Frisch, G. W. Trucks, H. B. Schlegel, G. E. Scuseria, M. A. Robb, J. R. Cheeseman, G. Scalmani, V. Barone, B. Mennucci, G. A. Petersson, H. Nakatsuji, M. Caricato, X. Li, H. P. Hratchian, A. F. Izmaylov, J. Bloino, G. Zheng, J. L. Sonnenberg, M. Hada, M. Ehara, K. Toyota, R. Fukuda, J. Hasegawa, M. Ishida, T. Nakajima, Y. Honda, O. Kitao, H. Nakai, T. Vreven, J. A. Montgomery Jr., J. E. Peralta, F. Ogliaro, M. Bearpark, J. J. Heyd, E. Brothers, K. N. Kudin, V. N. Staroverov, R. Kobayashi, J. Normand, K. Raghavachari, A. Rendell, J. C. Burant, S. S. Iyengar, J. Tomasi, M. Cossi, N. Rega, J. M. Millam, M. Klene, J. E. Knox, J. B. Cross, V. Bakken, C. Adamo, J. Jaramillo, R. Gomperts, R. E. Stratmann, O. Yazyev, A. J. Austin, R. Cammi, C. Pomelli, J. W. Ochterski, R. L. Martin, K. Morokuma, V. G. Zakrzewski, G. A. Voth, P. Salvador, J. J. Dannenberg, S. Dapprich, A. D. Daniels, Ö. Farkas, J. B. Foresman, J. V. Ortiz, J. Cioslowski, D. J. Fox. *Gaussian09, revision B.01*, Gaussian, Inc., Wallingford, CT (2010).
45. G. Jones, W. R. Jackson, C.-Y. Choi, W. R. Bergmark. *J. Phys. Chem.* **89**, 294 (1985).
46. E. Austin, M. Gouterman. *Bioinorg. Chem.* **9**, 281 (1978).
47. N. Ito, S. Arzhantsev, M. Maroncelli. *Chem. Phys. Lett.* **396**, 83 (2004).
48. S. Arzhantsev, H. Jin, G. A. Baker, M. Maroncelli. *J. Phys. Chem. B* **111**, 4978 (2007).
49. H. Jin, G. A. Baker, S. Arzhantsev, J. Dong, M. Maroncelli. *J. Phys. Chem. B* **111**, 7291 (2007).
50. R. S. Fee, M. Maroncelli. *Chem. Phys.* **183**, 235 (1994).
51. A. Paul, A. Samanta. *J. Phys. Chem. B* **111**, 4724 (2007).
52. W. Schuddeboom, S. A. Jonker, J. M. Warman, U. Leinhos, W. Kuhnel, K. A. Zachariasse. *J. Phys. Chem.* **96**, 10809 (1992).
53. D. Rappoport, F. Furche. *J. Am. Chem. Soc.* **126**, 1277 (2004).
54. J. Karpiuk. *J. Phys. Chem. A* **108**, 11183 (2004).
55. E. M. Kosower. *Acc. Chem. Res.* **15**, 259 (1982).
56. C. F. Chapman, R. S. Fee, M. Maroncelli. *J. Phys. Chem.* **99**, 4811 (1995).
57. K. S. Mali, G. B. Dutt, T. Mukherjee. *J. Chem. Phys.* **123**, 174504 (2005).
58. P. K. Mandal, M. Sarkar, A. Samanta. *J. Phys. Chem. A* **108**, 9048 (2004).
59. P. K. Mandal, A. Paul, A. Samanta. *J. Photochem. Photobiol., A* **182**, 113 (2006).

